Received: 31 May 2020 | Revised: 6 July 2020 | Accepted: 7 July 2020

DOI: 10.1002/pol.20200382

ORIGINAL ARTICLE

JOURNAL OF POLYMER SCIENCE WILEY

Silica-PMMA hairy nanoparticles prepared via phase transfer-assisted aqueous miniemulsion atom transfer radical polymerization

Dung-Yi Wu | **Florian Käfer** | **Nicholas Diaco** | **Christopher K. Ober**

Department of Materials Science and Engineering, Cornell University, Ithaca, New York

Correspondence
Christopher K. Ober, Department of Materials Science and Engineering, Cornell University, Ithaca, NY 14850, USA.
Email: c.ober@cornell.edu

Funding information
Air Force Office of Scientific Research, Grant/Award Number: AFOSR FA9550-17-1-0038; National Science Foundation, Grant/Award Numbers: DMR-1905403, NNCI-1542081, DMR-1719875; Cornell Center for Materials Research; Air Force Research Laboratory

Abstract

Hairy nanoparticles (HNPs) constitute a class of hybrid nanocomposites that are resistant to aggregation and agglomeration, although the green, large-scale synthesis of HNPs remains a challenge. In this work, 25 nm-diameter silica-core HNPs with a poly(methyl methacrylate) (PMMA) shell were synthesized using a graft-from approach in aqueous miniemulsion, employing atom transfer radical polymerization with activators regenerated by electron transfer (ARGET-ATRP). In particular, this work used tetrabutylammonium bromide (TBAB)-assisted phase transfer of monomer, markedly improving upon earlier methods by showing that phase transfer could take place in the absence of organic solvents. Furthermore, syntheses with selected monomer addition rates produced HNP graft densities ranging from 0.011 to 0.017 chains/nm^2 and shell thicknesses ranging from 2.5 to 11 nm. Finally, analysis of reaction kinetics revealed that shell growth reached completion in as little as 2 hr, confirmed by the synthesis of >1 g of PMMA-shell HNPs in a reduced timeframe.

KEYWORDS

aqueous miniemulsion, atom transfer radical polymerization, hairy nanoparticles, organic–inorganic hybrid, phase transfer

1 | INTRODUCTION

Organic–inorganic hybrid nanomaterials have been widely studied for their ability to combine the functional properties of vastly different materials.[1] For instance, inorganic nanoparticles can lend optical, mechanical, electronic, and other functional properties to hybrid particle-matrix blends, enhancing performance for a wide variety of applications.

Hairy nanoparticles (HNPs) are a particularly promising class of hybrid nanomaterial. An HNP consists of a small, inorganic core with an outer shell formed from grafted polymer chains. HNPs are unique in their capacity to resist the aggregation and agglomeration inherent to traditional hybrid blends, allowing a wide array of processing methods to be used without losing the intended functionality of the composite.[2] HNPs also exhibit many practical features, such as chain entanglement with neighboring particles in addition to self-assembly in a wide variety of conditions.[3] These unique properties, among others, have already been exploited for applications including sensing, photonics, and catalysis.[4,5]

Forming well-defined assemblies of HNPs and studying structure–property relationships requires precise control of particle size, polymer molecular weight, and chain graft density. Of the methods known for synthesizing HNPs, the greatest structural control is afforded by using a

This article was published online on 14th August 2020. A minor error in Scheme S1 and an error in Figure S1 in the supporting information were subsequently identified. This notice is included to indicate that these were corrected on the 15th February 2021.

"graft-from" approach, in which initiators are grafted to the surfaces of bare nanoparticles, followed by surface-initiated polymerization.[6] HNP synthesis using a graft-from approach is often performed via atom transfer radical polymerization (ATRP), a common and versatile method for creating well-defined polymeric structures.[7,8] For instance, Werne et al used surface-initiated ATRP in bulk monomer to achieve the controlled growth of silica-core HNPs with polystyrene (PS) and poly(methyl methacrylate) (PMMA) shells.[6,9] In a similar fashion, Pyun et al used ATRP to synthesize silica-core HNPs with well-defined shells consisting of PS, PMMA, and poly(n-butyl acrylate) (PBA) homopolymers and copolymers, highlighting the versatility of this approach.[10]

While these approaches demonstrate the high degree of flexibility in designing HNP shells, a water-based, green synthesis would be preferable for scaling up HNP production in an eco-friendly fashion.[11] Unlike the methods employed in the studies described above, ATRP can be performed in water-based systems by using electron transfer reactions to generate polymerization activators.[12] This variation on ATRP was further refined by using activators regenerated by electron transfer (ARGET-ATRP), which made synthesis more eco-friendly by drastically reducing the amount of metal catalyst needed.[13,14] These advances allowed for the green, scalable synthesis of PBA-shell HNPs via ATRP in aqueous miniemulsion.[15] Despite the progress made on these fronts, however, there is still a desire for a versatile, water-based method for synthesizing HNP shells with a broad variety of monomeric precursors.

Recently, Cordero et al developed a scheme for performing ARGET-ATRP in aqueous emulsion by using a tetrabutylammonium bromide (TBAB) salt as a phase transfer agent to shuttle hydrophobic ATRP catalyst complexes between micelles and the aqueous phase.[7] In this work, Cordero et al's method is extended to the synthesis of PMMA-shell HNPs from 25 nm silica nanoparticle cores by using graft-from ATRP in miniemulsion with a nonionic surfactant (Scheme 1). Although versatile, the technique reported by Cordero et al promoted phase transfer of the monomer by using acetone, which is undesirable for scalable, green reactions. In this work, it is found that polymerization can take place in the absence of acetone, and it is further shown that acetone-free conditions eliminate unwanted side products. Furthermore, by varying monomer addition rates, it is found that HNP shell properties such as graft density, molecular weight, and shell thickness can be fine-tuned. This work provides a feasible method for the green, scalable synthesis of a variety of HNP shells.

2 | EXPERIMENTAL

2.1 | Materials

Copper (II) bromide (99%, extra pure, anhydrous), methyl methacrylate (MMA) (stabilized), L (+)-ascorbic acid, TBAB (99%), aluminum oxide (basic), and dimethylethoxysilane (94 wt%) were purchased from Acros Organics and used as received. Triethylamine, 2-bromoisobutyryl

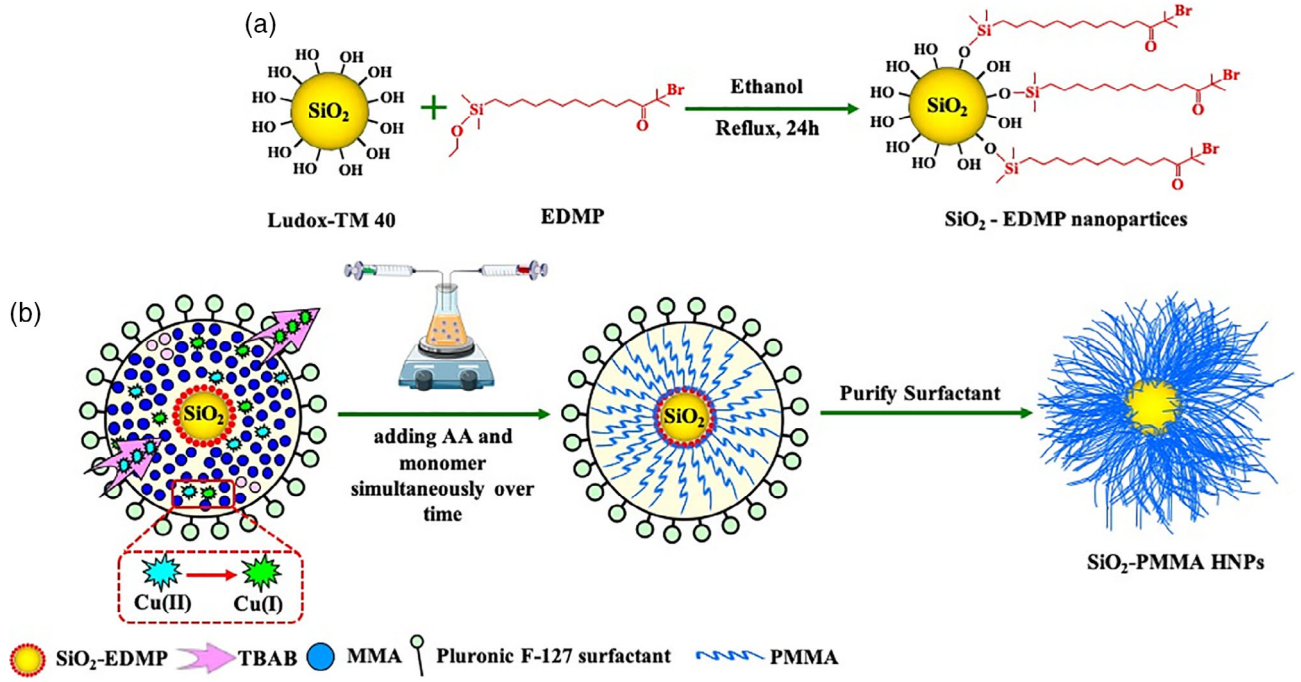

SCHEME 1 (a) Preparation of EDMP-functionalized SiO_2 nanoparticles. (b) Synthesis of SiO_2-PMMA HNPs using miniemulsion ARGET-ATRP (polymer shell enlarged for illustrative purposes) [Color figure can be viewed at wileyonlinelibrary.com]

bromide (BIBB), $Pt_2[(Me_2SiCH{=}CH_2)_2O]_3$ (Karstedt's catalyst) in water, Pluronic F-127, 28% NH_3, and Ludox TM-40 particles were purchased from Sigma–Aldrich and used as received. Tris(2-pyridylmethyl) amine (TPMA, 98 wt%) was purchased from TCI. Ammonium hydroxide (28 wt%), hydrochloric acid (36.5–38.0 wt%), Dowex 50 W X8 100–200 mesh, Dowex 1X8-200 mesh ion-exchange resin, and 10 k MW cut-off 35 mm Snakeskin dialysis tubing were purchased from Fisher Chemical. The deionized water used in all experiments was obtained from a MilliporeSigma Milli-Q IQ 7000 Ultrapure Water System with a resistance of 18.2 MΩ.

2.2 | Synthesis of EDMP

The synthesis of the ATRP initiator, 11-(ethoxydimethylsilyl) undecyl 2-bromo-2-methylpropanoate (EDMP), was carried out in two steps (Scheme S1). Step 1 (bromination): 10-undecen-1-ol (4.257 g, 25 mmol) and pyridine (2.1 ml, 26 mmol) were dissolved in 30 ml of anhydrous tetrahydrofuran (THF) in a 100 ml round-bottom flask. 2-bromoisobutyryl bromide (BIBB) (5.760 g, 24 mmol, in 10 ml THF) was added dropwise over 2 hr, while stirring in an ice bath. After 2 hr, the ice bath was removed and the solution was subsequently stirred for 24 hr at 25°C. Afterwards, the precipitate was filtered off and THF was removed under reduced pressure to obtain a yellow oil. The crude product was washed twice with dichloromethane (DCM) and saturated Na_2CO_3. DCM was removed under reduced pressure, then the crude product was dried using Na_2SO_4 and purified using column chromatography with DCM to obtain a pale-yellow oil (95% yield). Step 2 (hydrosilylation): Karstedt's catalyst (6 μl, 11 μmol) and dimethylethoxysilane (8.9 g, 85.4 mmol) were added to the product from step 1 (1.28 g, 4 mmol). The mixture was stirred overnight at room temperature under a nitrogen atmosphere. After removing the excess dimethylethoxysilane under reduced pressure, the resulting EDMP was stored at 20°C. The synthesized EDMP was characterized by ^{1}H NMR (Figure S1). Peaks appeared at δ = 0.21 (Si—CH_3); 0.61 (—CH_2—CH_2—Si—); 1.21 (—CH_2—CH_3); 1.23–1.60 (polymer backbone, —CH_2—); 2.02 (—C[CH_3]$_2$Br); 3.83, 4.13 (—O—CH_2 —CH_2—) ppm.

2.3 | Pretreatment of Ludox TM-40 silica particles

Ludox TM-40 particles were pretreated with Dowex resins to replace surface ions with hydroxyl groups, allowing for subsequent surface functionalization. First, each of Dowex 50 W X8 and Dowex 1X8 (both 50 g) were transferred to separate 600 ml beakers. The resins were washed with 3 N NaOH, hot water, methanol, and cold water. After each individual wash, the resins were collected by filtration. This washing cycle was repeated 5 times for both resins. After the last wash cycle of Dowex 50 W X8, the resin was converted to the hydrogen form by a final washing step using an excess amount of a 3 N HCl solution. Similarly, Dowex 1X8 was converted to the hydroxy form shortly before use with a 3 N NaOH solution. Next, the Ludox TM-40 silica particle dispersion (100 ml) was diluted with 100 ml of Milli-Q water, stirred, and added to Dowex 50 W X8 resin in a beaker and agitated overnight. Ludox TM-40 particles were then collected via filtration and added to Dowex 1X8 resin in a beaker and stirred overnight. The particles were then collected via filtration, with large aggregates centrifuged down at 3000 rpm, then dialyzed against ethanol for 1 week. Next, the Ludox TM-40 silica particle dispersion (100 ml) was diluted with 100 ml of Milli-Q water, stirred, and added to Dowex 50 W X8 resin in a beaker and agitated overnight. Ludox TM-40 particles were then collected via filtration and added to Dowex 1X8 resin in a beaker and stirred overnight. The particles were then collected via filtration, with large aggregates centrifuged down at 3000 rpm, then dialyzed against ethanol for 1 week.

2.4 | Preparation of EDMP-functionalized Ludox TM-40 particles

In the first step of attaching ATRP initiators to the silica particle surfaces (Scheme 1(a)), pretreated Ludox TM-40 silica particles were dispersed in ethanol (1 g, 50 ml) and added to a 200 ml round-bottom flask. Afterward, a pH of 10 was obtained by the addition of 28% NH_3 solution. EDMP (0.860 g, 0.002 mol) was then slowly added to the dispersion and refluxed for 24 hr at 85°C. Finally, the particles were purified by dialysis against ethanol for 1 week, freeze-dried, and stored at 4°C with minimal humidity. The amount of grafted EDMP was determined by TGA, see Figure S2.

2.5 | Synthesis of Silica-PMMA HNPs

EDMP-functionalized SiO_2 nanoparticles (200 mg) were mixed with 10 ml of a Pluronic F-127 (0.04 g/ml) solution in a 20 ml scintillation vial and vortexed and sonicated until a milky white suspension was formed. In parallel, TBAB (1.934 g, 6 mmol), $CuBr_2$ (1 mg, 4.48 μmol), tris (2-pyridylmethyl) amine (TPMA) (12.2 mg, 42 μmol), and water (43.2 ml) were added in a 100 ml round-bottom flask with a stirring bar. The particle suspension was

added to the 100 ml flask and degassed for 20 min by bubbling with argon. After removing the stabilizer via vacuum distillation, MMA (7.5–14.1 mmol/hr) and an aqueous solution of ascorbic acid (2.27 mM, 3.6 ml, 1.4 μmol/hr) were added to the 100 ml flask simultaneously over the course of 6 hr using two syringe pumps (Scheme S2). In cases, where the syringe pumping rate was not precise enough to add the exact amount of MMA desired during the reaction, the pumping rate was adjusted so that all monomer would be added a short time before the reaction was terminated. After 6 hr, at which point the addition of both MMA and ascorbic acid was complete, the polymerization was terminated by opening the reaction flask to air. The HNPs were separated by centrifuging at 4400 rpm for 20 min, washed twice with THF and Milli-Q water, and dried in a vacuum oven at 80°C (Scheme 1(b)). The polymer content of the synthesized HNPs was determined by TGA, see Figure S3.

2.6 | Analytical procedures

Fourier transform infrared spectroscopy (FTIR) measurements were performed on a Vertex V80V vacuum FTIR instrument; Bruker, Billerica, MA. Samples analyzed with FTIR were first ground into a fine powder. Spectrum were acquired at 2 cm^{-1} resolution in the range of 4,000–400 cm^{-1} with an integrating time of 1 min for each sample. Thermogravimetric analysis (TGA) measurements were performed on a TA Instruments Inc. TGA Q500, heating the samples from 20 to 600°C with a heating rate of 10°C/min under a nitrogen atmosphere. The mass of the samples for each measurement was in the range of 8–10 mg. The molar mass of the grafted polymer chains were obtained after HF etching by using a Waters ambient temperature THF-GPC. A Waters 410 - differential refractive index detector and a Waters 486,106 UV/vis detector were applied in parallel. The three GPC columns used are PSS (Polymer Standards Service) SDV models with 8 × 300 mm dimensions, with porosities of 50 Å, 500 Å, and Linear M. Elugrams were obtained at 35°C using a THF flow rate of 1 ml/min and were calibrated with narrow polystyrene standards. The molar mass was analyzed using the Breeze software. NMR spectrum were measured using a Varian INOVA-500 NMR Spectrometer in $CDCl_3$ at 20°C with an HBB nanoprobe, and the data was recorded using the VNMR 6.1C software. XRD measurements of the HNPs were carried out on Bruker-D8 Advance ECO powder diffractometer. Diffraction was measured using Cu K-α radiation with a wavelength of approximately $\lambda = 1.54$ Å and photon energy of 8.04 keV. The source of the 40 kV × 25 mA X-rays was a water-cooled fixed Cu target excited by an electron gun. Transmission electron microscope (TEM) images were collected by an FEI F20 TEM STEM with a Thermo-Fisher GF20 scope, monochromated and operated at 200 kV. Samples were suspended in tetrahydrofuran and deposited on carbon plated grids. The images were acquired in High Angular Annular Darkfield (HAADF) mode TEM. Dynamic light scattering (DLS) measurements in water were performed with a Malvern Zetasizer Nano ZS90.

3 | RESULTS AND DISCUSSION

In general, the synthesis of HNPs was carried out in two steps. In the first step, Ludox TM-40 silica particles with a diameter of 25 nm were functionalized with the ATRP initiator EDMP, as shown in Scheme 1(a). Notably, the hydrophobic initiator EDMP was used in order to localize all polymerization steps within the monomer phase for better reaction control. After surface-functionalization, the second step involved adding the now hydrophobic nanoparticles to a heated reaction flask with Pluronic F-127 surfactant, forming a micellar particle suspension stable enough for hydrophobic polymer chains to be grown from the SiO_2 surface with minimal particle aggregation. The synthesis of PMMA shells from the functionalized SiO_2 nanoparticle surfaces via ARGET-ATRP in miniemulsion is the primary object of this research and is discussed in detail below.

The polymerization scheme described herein was based on the technique of Cordero et al, wherein TBAB and acetone played a role in monomer and catalyst transport.[7] In particular, Cordero et al used TBAB, which has a finite solubility in both the oil and aqueous phases, as a phase transfer agent to help to shuttle monomer and ATRP catalyst complex into the micelles. Furthermore, Cordero et al introduced acetone in the miniemulsion ARGET-ATRP of MMA to both increase the solubility of monomer in the aqueous phase and assist in the diffusion of monomer into the micellar oil phase, thereby localizing polymerization in the micelles.[16] Since the use of acetone is undesirable for green, scalable syntheses, the present work further investigates the roles of TBAB and acetone for producing PMMA-shell HNPs.

To investigate the roles of TBAB and acetone in HNP synthesis, a constant MMA concentration of 0.67 mol/L was added to the reaction flask at the beginning of each of three separate reactions (Table 1, Samples 1–3). The reaction in Sample 1 was conducted with only TBAB; the reaction in Sample 2 was conducted with both TBAB and 20 vol% acetone; and the reaction in Sample 3 was performed with only 20 vol% acetone. As shown in Table 1, it was observed that the inclusion of acetone leads to generally higher polymer content in the resulting

TABLE 1 SiO_2-PMMA HNPs synthesized using mini-emulsion ARGET-ATRP

Sample	MMA (mol/L)	MMA feeding rate (mmol/hr)	Polymer content (wt%)	Graft density (chains/nm^2)	Molar mass	Shell thickness (nm)[a]
1[b]	0.67	—	32	0.0084	214,300	—
2[b, c]	0.67	—	50	0.013	328,700	—
3[b, c, d]	0.67	—	53	0.029	158,600	—
4	0.67	7.5	21	0.011	86,400	2.5 ± 0.3
5	1	10.3	25	0.011	106,200	7.0 ± 1.0
6	1.17	12.2	32	0.017	105,800	11.0 ± 1.6
7	1.34	14.1	61	0.024	276,300	—

[a]The diameters of SiO_2-PMMA HNPs were determined by averaging the diameters of 10 particles measured by TEM and analyzed with ImageJ.
[b]All MMA was added at the beginning of the sample.
[c]With 20 vol% acetone.
[d]Without TBAB.

HNPs, compared with the results of TBAB alone. The polymer graft density, calculated according to Equation S1, was also higher for both reactions containing acetone. A possible explanation for this difference is that the acetone-assisted transfer of monomer results in the increase of initial MMA concentration located inside the micelles, leading to a higher initial number of growing chains. The trend for the molecular weight of grafted polymers is less clear, but TBAB alone results in a value of M_n intermediate between those of acetone alone and TBAB + acetone.

An additional factor that must be taken into account is the amount of ungrafted free polymer found in the reaction flask after the synthesis, measured as a weight fraction of the total amount of monomer added. The presence of ungrafted polymer chains can result from several pathways, including chain transfer reactions, residual ungrafted EDMP, or chain scission due to hydrolysis or shear during processing.[15] In general, the presence of free polymer is undesirable, since it lowers yield and reaction purity. For Sample 1 containing only TBAB, free polymer was present at 20 wt%, whereas for Samples 2 and 3 containing 20 vol% acetone, free polymer was measured at 40 wt% and 36 wt%, respectively (Table S1). The higher amounts of ungrafted polymer produced when acetone is present, coupled with the fact that acetone leads to only slight changes in shell characteristics, means that the use of TBAB alone is preferable for a scalable, green synthetic system. Thus, for the remainder of the experiments described, acetone was excluded from the reaction and TBAB alone was used.

The rate of monomer addition was observed to play an important role in reaction control. For instance, Samples 1 and 4 in Table 1 share the same final concentration of added MMA, but the MMA was added all at once for Sample 1 and over the course of the whole reaction for Sample 4. Although the HNPs in Sample 1 - possessed greater polymer content and the chains had a higher molar mass than those of Sample 4, Sample 4 had no measurable free polymer present at the end of the reaction, compared with 20 wt% free polymer found in the Sample 1 reaction flask. Similarly, Samples 5 and 6 contained no measurable quantities of free polymer (Table S1). This suggests that slowly adding MMA over the course of the reaction limits the mechanisms responsible for the formation of ungrafted polymer, since, for instance, one might expect a lower monomer concentration at any given time to limit chain transfer.

After the presence of grafted PMMA chains on the SiO_2 particle surfaces was confirmed using FTIR (Figure S4) and XRD (Figure S5) measurements, darkfield TEM measurements of the PMMA-shell HNPs were made to characterize particle geometry via measurements of diameter and shell thickness. The TEM images of the HNPs described in Table 1, Samples 4–7 are shown in Figure 1. As shown in Figure 1, the HNPs exhibit a spherical core-shell morphology with tunable PMMA shell thickness. Shell thickness was calculated by subtracting the core radius from the outer radius of individual HNPs as viewed in TEM, then averaging to get a value for the whole sample. As might be expected, increasing MMA concentrations led to thicker PMMA shells until the onset of aggregation at a final MMA concentration of 1.34 mol/L, as seen for Sample 7 in Figure 1(d, h), showing large 200–300 nm aggregates. The aggregates in Sample 1 (Figure S6) and the 16 wt% free polymer in Sample 7 (Table S1) suggest that the presence of free polymer may cause this aggregation.

For Samples 4–6 in Table 1, on the other hand, minimally aggregated particles with shell thicknesses of 2.5 ± 0.3, 7.5 ± 1.0, and 11.0 ± 1.6 nm (Figure 1(a-c); (e-g)), respectively, were observed. These values were

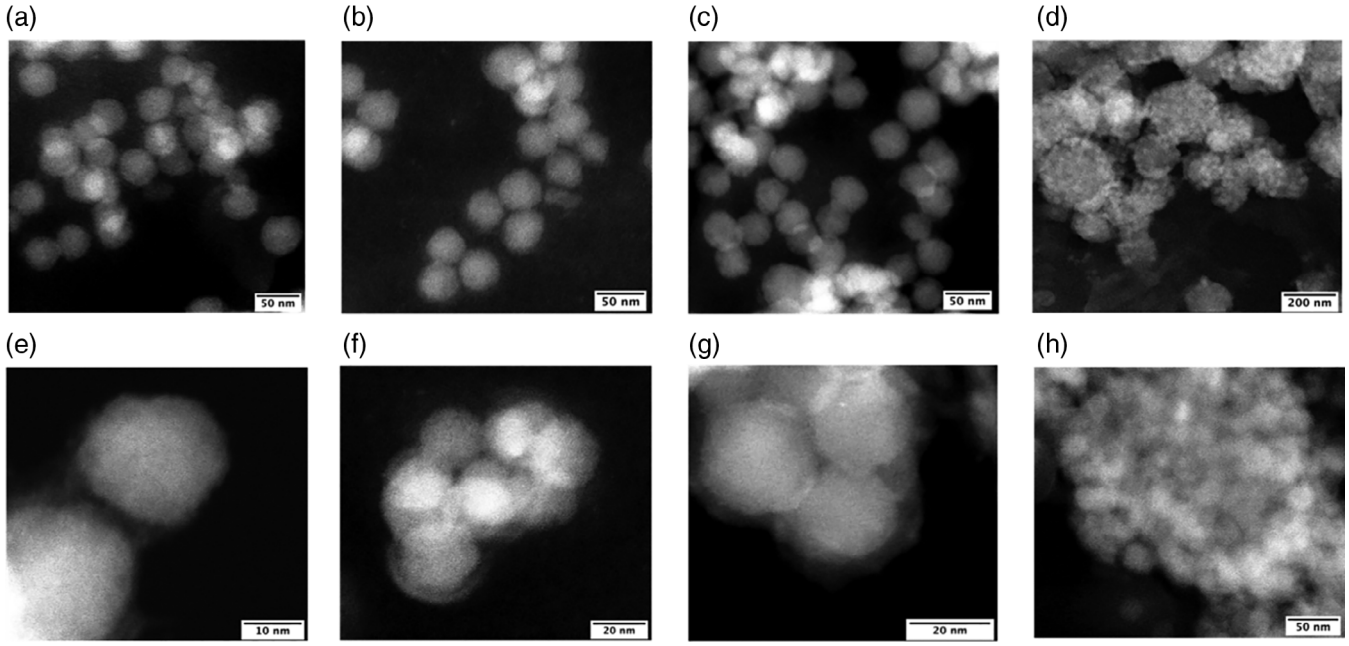

FIGURE 1 TEM images of the SiO_2-PMMA HNPs obtained via miniemulsion ARGET-ATRP with selected polymer content (Table 1, Samples 4–7). (a, e) Sample 4. (b, f) Sample 5. (c, g) Sample 6. (d, h) Sample 7

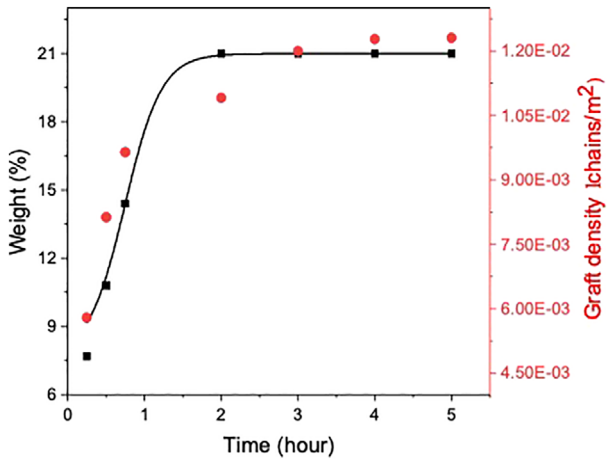

FIGURE 2 Polymerization kinetics for the grafting of MMA from silica nanoparticles in miniemulsion ARGET-ATRP. MMA = 0.67 mol/L; MAA feeding rate = 7.5 mmol/hr at 80°C. The curves are drawn as a guide to the eye, rectangle (Weight (%)), circle (Graft density (Chains/nm^2)) [Color figure can be viewed at wileyonlinelibrary.com]

similar to those found with DLS, which gave shell thicknesses of approximately 4.5, 6, and 10 nm, respectively (-Figure S7). These observations demonstrate that shell thickness can be tuned by varying the MMA addition rate, although for high enough MMA concentrations HNP aggregation may occur.

In order to qualitatively understand the time-dependence of the polymer grafting process, a study of polymerization kinetics was performed by regularly extracting samples from a reaction using the same conditions described for Sample 4 in Table 1. The results of this experiment are shown in Figure 2. The molar mass and polymer weight content of the HNPs increased for approximately 2 hr, then became constant at approximate values of M_n = 78,000 and 21 wt%, respectively, consistent with the results of Sample 4. As a result, the polymer graft density calculated according to Equation S1 reached a value of 0.011 chains/nm^2 at 2 hr and remained approximately constant for the remainder of the reaction. To verify that the reaction neared completion at around 2 hr, an experiment was performed to synthesize over 1 g of PMMA-shell HNPs using the reaction conditions of Sample 6. Analysis of this reaction was nearly identical to that of Sample 6 and suggested minimal to no occurrence of ungrafted PMMA. Furthermore, the resulting particles had homogeneous shells and a low degree of aggregation, demonstrating the scalability of the synthetic methods described herein.

4 | CONCLUSION

It was shown that miniemulsion ARGET-ATRP using the phase transfer agent TBAB, as originally developed by Cordero et al, could be adapted to the synthesis of 25 nm silica-core, PMMA-shell HNPs in aqueous media. Unlike Cordero et al's method, however, it was found that the HNP shell synthesis could be performed without acetone,

thereby eliminating the use of organic solvents. Furthermore, by changing the monomer feeding rate it was found that free polymer formation could be eliminated while also giving control of the HNPs' graft density and shell thickness, which ranged from 0.011 to 0.017 chains/nm^2 and 2.5 to 11 nm, respectively. A study of reaction kinetics revealed that although the reaction took place over the course of 6 hr, the HNP graft density remained relatively constant after 2 hr. To demonstrate the feasibility of large-scale reactions over compressed timeframes, a gram-scale, 2-hr reaction was successfully performed, resulting in HNPs with characteristics similar to those from the smaller-scale, 6-hr reactions. While future work will focus on extending this method to synthesize HNP shells of varying materials and morphologies, this work demonstrates the feasibility of using a phase transfer agent and varied monomer feeding rates to aid in the green, scalable synthesis of finely controlled HNPs.

ACKNOWLEDGMENTS

The authors would like to extend their gratitude to the Air Force Office of Scientific Research (AFOSR FA9550-17-1-0038), and also to the Air Force Research Laboratory for prior support. This work was performed in part at the Cornell NanoScale Facility, a member of the National Nanotechnology Coordinated Infrastructure (NNCI), which is supported by the National Science Foundation (Grant NNCI-1542081). This work made use of the Cornell Center for Materials Research Shared Facilities, which are supported through the NSF MRSEC program (DMR-1719875). DLS measurements were made using facilities provided by the Cornell Energy Systems Institute (CESI). Discussions with Dr Richard Vaia and Dr Allen Schantz were invaluable to the success of this research.

ORCID

Dung-Yi Wu https://orcid.org/0000-0002-3749-9429
Florian Käfer https://orcid.org/0000-0003-4988-3812
Nicholas Diaco https://orcid.org/0000-0001-8766-7075
Christopher K. Ober https://orcid.org/0000-0002-3805-3314

REFERENCES

[1] V. P. Ananikov, *Nanomaterials* **2019**, *9*, 1197.
[2] H. Koerner, L. F. Drummy, B. Benicewicz, Y. Li, R. A. Vaia, *ACS Macro Lett.* **2013**, *2*, 670.
[3] A. Chremos, J. F. Douglas, *Soft Matter* **2016**, *12*, 9527.
[4] M. Kohri, K. Uradokoro, Y. Nannichi, A. Kawamura, T. Taniguchi, K. Kishikawa, *Photonics* **2018**, *5*, 36.
[5] C. Chen, D. Y. W. Ng, T. Weil, *Mater. Chem. Front.* **2019**, *3*, 1449.
[6] T. von Werne, T. E. Patten, *J. Am. Chem. Soc.* **1999**, *121*, 7409.
[7] R. Cordero, A. Jawaid, M.-S. Hsiao, Z. Lequeux, R. A. Vaia, C. K. Ober, *ACS Macro Lett.* **2018**, *7*, 459.
[8] P. Pasetto, H. Blas, F. Audouin, C. Boissière, C. Sanchez, M. Save, B. Charleux, *Macromolecules* **2009**, *42*, 5983.
[9] T. von Werne, T. E. Patten, *J. Am. Chem. Soc.* **2001**, *123*, 7497.
[10] J. Pyun, S. Jia, T. Kowalewski, G. D. Patterson, K. Matyjaszewski, *Macromolecules* **2003**, *36*, 5094.
[11] K. Landfester, *Angew. Chem., Int. Ed.* **2009**, *48*, 4488.
[12] K. Min, H. Gao, K. Matyjaszewski, *J. Am. Chem. Soc.* **2005**, *127*, 3825.
[13] W. Jakubowski, K. Min, K. Matyjaszewski, *Macromolecules* **2006**, *39*, 39.
[14] K. Matyjaszewski, N. V. Tsarevsky, *J. Am. Chem. Soc.* **2014**, *136*, 6513.
[15] L. Bombalski, K. Min, H. Dong, C. Tang, K. Matyjaszewski, *Macromolecules* **2007**, *40*, 7429.
[16] J. Ugelstad, K. H. Kaggerud, F. K. Hansen, A. Berge, *Die Makromol. Chem.* **1979**, *180*, 737.

SUPPORTING INFORMATION

Additional supporting information may be found online in the Supporting Information section at the end of this article.

How to cite this article: Wu D-Y, Käfer F, Diaco N, Ober CK. Silica-PMMA hairy nanoparticles prepared via phase transfer-assisted aqueous miniemulsion atom transfer radical polymerization. *J Polym Sci.* 2020;58:2310–2316. https://doi.org/10.1002/pol.20200382